with that of a major paracrine effector of normal epithelial cell proliferation.

REFERENCES AND NOTES

1. R. James and R. A. Bradshaw, *Annu. Rev. Biochem.* **53**, 259 (1984).
2. A. Miyajima *et al.*, *FASEB J.* **2**, 2462 (1988).
3. J. S. Rubin *et al.*, *Proc. Natl. Acad. Sci. U.S.A.* **86**, 802 (1989).
4. Two 26-bp oligonucleotide probes were synthesized on the basis of the amino acid sequence Asn-Asp-Met-Thr-Pro-Glu-Gln-Met-Ala, determined by microsequencing of purified KGF. One probe contained all possible codon combinations for the amino acids, whereas the other contained inosine residues at the degenerate third positions of the codons for Thr and Pro, to reduce the redundancy from 256 to 16. Pools of deoxyoligonucleotides (50 pmol) were 5′ end–labeled with 83 pmol of [γ-^{32}P]ATP (3000 Ci/mmol, Amersham) and 10 units of T4 polynucleotide kinase. The recombinant phages were replica-plated onto nitrocellulose filters and hybridized overnight at 42°C with ^{32}P-labeled deoxyoligonucleotides in 20% formamide, 10% Dextran sulphate, 10 m*M* tris-HCl (*p*H 7.5), 8× standard saline citrate (SSC), 5× Denhardt's solution, and denatured salmon sperm DNA (50 μg/ml). Filters were washed in 0.5× SSC and 0.1% SDS at 50°C and exposed to Kodak X-Omat AR film.
5. The nucleotide sequence of the KGF cDNA was determined by the dideoxy chain-termination method [F. Sanger *et al.*, *Proc. Natl. Acad. Sci. U.S.A.* **74**, 54 (1977)] of overlapping restriction fragments that had been subcloned into pUC vectors [C. Yanisch-Perron *et al.*, *Gene* **33**, 103 (1985)].
6. M. Kozak, *Nucleic Acids Res.* **15**, 8125 (1987).
7. D. J. Lipman and R. W. Pearson, *Science* **227**, 1435 (1985).
8. K. Thomas, *FASEB J.* **1**, 434 (1987).
9. X. Zhan, B. Bates, X. Hu, M. Goldfarb, *Mol. Cell. Biol.* **8**, 3487 (1988); M. Taira *et al.*, *Proc. Natl. Acad. Sci. U.S.A.* **84**, 2980 (1987); P. Delli-Bovi and C. Basillico, *ibid.*, p. 5660.
10. A. Jakobovits, G. M. Shackleford, H. E. Varmus, G. R. Martin, *Proc. Natl. Acad. Sci. U.S.A.* **83**, 7806 (1986); G. Peters, S. Brookes, S. Dickson, *Cell* **33**, 364 (1983).
11. G. von Heijne, *Nucleic Acids Res.* **14**, 4683 (1986).
12. M. Jaye *et al.*, *Science* **233**, 541 (1986); J. A. Abraham *et al.*, *ibid.*, p. 545.
13. R. Moore *et al.*, *EMBO J.* **5**, 919 (1986).
14. Total cellular RNAs were isolated by cesium trifluoroacetate (Pharmacia) gradient centrifugation. Poly(A)$^+$ RNA (5 μg) [H. Aviv and P. Leder, *Proc. Natl. Acad. Sci. U.S.A.* **69**, 1408 (1972)] was denatured and subjected to electrophoresis in 1% formaldehyde gels. After mild alkali denaturation (50 m*M* NaOH for 30 min), RNA was transferred to nitrocellulose filters with 1*M* ammonium acetate as a convectant. The cDNA probes were ^{32}P-labeled by nick translation and hybridized to filters in 50% formamide, 10% Dextran sulfate, 10 m*M* tris (*p*H 7.5), 5× SSC, 2.5× Denhardt's solution, and denatured salmon sperm DNA (50 μg/ml). Filters were washed in 0.1× SSC and 0.1% SDS at 50°C and exposed.
15. S. L. Mansour and G. R. Martin, *EMBO J.* 7, 2035 (1988).
16. G. Shaw and R. Kamen, *Cell* **46**, 659 (1986).
17. P. Finch and S. A. Aaronson, unpublished results.
18. B. E. Weissman and S. A. Aaronson, *Cell* **32**, 599 (1983).
19. H. Bloemendal *et al.*, *Ann. N.Y. Acad. Sci.* **455**, 95 (1985); S. Ferrari *et al.*, *Mol. Cell. Biol.* **6**, 3614 (1986); the probe was a Hinc II–Dra III fragment spanning nucleotides 922 to 1708 of the human vimentin cDNA.
20. D. R. Roop *et al.*, *J. Invest. Dermatol.* **81**, 144s (1983); D. R. Roop *et al.*, *Cancer Res.* **48**, 3245 (1988); the cDNA probe, specific for the K1 transcript, was an Eco RI–Hind II fragment spanning ~400 nucleotides of the 3′ untranslated region.
21. R. H. Sawyer and J. F. Fallow, Eds., *Epithelial-Mesenchymal Interaction During Development* (Praeger, New York, 1983).
22. G. Carpenter and S. Cohen, *Annu. Rev. Biochem.* **48**, 193 (1979); R. Derynck, *Cell* **54**, 593 (1988); L. B. Rall *et al.*, *Nature* **313**, 228 (1985).
23. V. K. M. Han, A. J. D'Ercole, P. K. Lund, *Science* **236**, 193 (1987).
24. D. Gospodarowicz, G. Neufeld, L. Schweigerer, *J. Cell. Physiol.* **5**, 15 (1987).
25. T. A. Libermann *et al.*, *EMBO J.* **6**, 1627 (1987); G. D. Shipley, M. D. Sternfeld, R. J. Coffey, M. R. Pittelkow, *J. Cell. Biochem.* **12A** (suppl.), C420 (abstr.) (1988); P. Finch and S. A. Aaronson, unpublished results.
26. The KGF cDNA sequence may be requested from GenBank by accession number M25295.
27. Abbreviations for the amino acid residues are as follows: A, Ala; C, Cys; D, Asp; E, Glu; F, Phe; G, Gly; H, His; I, Ile; K, Lys; L, Leu; M, Met; N, Asn; P, Pro; Q, Gln; R, Arg; S, Ser; T, Thr; V, Val; W. Trp; and Y, Tyr.
28. R. K. Saiki *et al.*, *Science* **230**, 1350 (1985); probe B was derived from KGF cDNA (nucleotides 2781 to 3653). Amplification was performed with two 18-base oligonucleotide primers, and the amplified fragment was resolved on an agarose gel and recovered by electroelution.
29. Recently another member of the FGF gene family, designated *FGF-6*, was identified on the basis of homology to a human *hst* probe [I. Marics *et al.*, *Oncogene* **4**, 335 (1989)]; hence, KGF is the seventh member of the FGF family.
30. Hybridization with the human KGF and vimentin probes was performed in 40% formamide, 5× SSC, 2.5× Denhardt's solution, 10% Dextran sulphate, 25 m*M* sodium phosphate buffer (*p*H 6.5), and yeast transfer RNA (100 μg/ml) at 42°C. Filters were washed at 55°C with 1× SSC and 0.1% SDS for 30-min intervals. Hybridization with the mouse K1 probe was carried out under more stringent conditions in 50% formamide and the filters were washed at 60°C with 0.1× SSC and 0.1% SDS.

31. We thank J. Wong for assistance in RNA blot analysis, W. Weinberg and S. Yuspa for providing the mouse keratin probe, R. Baserga for providing the human vimentin cDNA, J. Lechner for providing the immortalized bronchial epithelial lines S6 and R1, M. Stampfer for providing the immortalized mammary epithelial line B5/589, M. Kraus and S. Rudikoff for helpful discussions, and S. R. Tronick for assistance in running DNA sequence analysis computer programs. Supported in part by a Japanese Overseas Cancer Fellowship from the Foundation for Promotion of Cancer Research to T.M.

16 March 1989; accepted 28 June 1989

Light Adaptation in Cat Retinal Rods

T. TAMURA, K. NAKATANI, K.-W. YAU

It has long been an open question whether individual rod receptors in the mammalian retina show any light adaptation. The prevailing evidence so far has suggested that these cells, unlike those in lower vertebrates, adapt little if at all. The experiments on cat rods reported here, however, indicate that this is not really true. Since the cone system in the cat retina has a fairly high light threshold, the rods also need to adapt so that they do not saturate with light before the cones fully take over vision at higher light intensities. In similar experiments, adaptation was found in rods of other mammalian species, including primates.

LIGHT ADAPTATION ALLOWS THE VISUAL system to maintain its ability to detect contrast despite large changes in the light level. Although this phenomenon has been well characterized in many ways, it is still not clear how much of light adaptation is at the "network" level (that is, resulting from synaptic interactions in the retina) and how much of it resides in the photoreceptors themselves (*1*). For rods, the receptors for dim light, there is overwhelming evidence in cold-blooded vertebrates that these cells can adapt to light (*2–6*). In mammals, however, the cumulative evidence has been against the existence of any rod adaptation (*1, 7, 8*). The most recent and direct evidence, on the basis of electrical recordings from single rods of the macaque monkey, has also indicated that these cells show negligible adaptation to light (*9*). Thus, there may be a fundamental difference in rod behavior between mammals and lower vertebrates and, perhaps more generally, between warm-blooded and cold-blooded animals (*10*). To further examine this question, we have studied single rods from the cat retina. Surprisingly, these cells showed clear evidence of light adaptation.

An eye was removed from a cat under pentobarbital anesthesia in dim red light. In infrared light and under physiological saline solution (*11*), the eye was coronally hemisected, and several small pieces of retina were removed from the posterior eyecup. These samples were stored at 5°C in Dulbecco's modified Eagle's medium (Gibco) for use over a period of ~10 hours. When needed, a piece of retina was transferred into physiological saline solution and finely chopped on a layer of cured Sylgard (Dow Corning). We then recorded membrane current from a single rod outer segment projecting from a retinal fragment, after sucking the outer segment into a glass pipette filled with the same saline and connected to a current-recording amplifier (*12*). This outer segment was stimulated transversely with diffuse, unpolarized light at 500 nm (*12*). The temperature in the immediate vicinity of the recorded cell was maintained at 38° to

Howard Hughes Medical Institute and Department of Neuroscience, The Johns Hopkins University School of Medicine, Baltimore, MD 21205.

40°C with an insulated heating filament.

A family of responses from a cat rod to steps of light at different intensities is shown in Fig. 1A. The low-frequency noise in the step responses was due to photon fluctuations. Normalized response-intensity relations measured at the early rising phase of the responses (at 100 and 150 ms, respectively, after the onset of light) are plotted in Fig. 1B. The two dashed curves have identical forms, but are simply displaced horizontally; they are drawn according to the relation (*6, 9, 13*):

$$\hat{r}_s = 1 - e^{-k_s I_s} \quad (1)$$

where $\hat{r}_s$ is the normalized response amplitude, k_s is a constant, and I_s is the light step intensity (in photons per square micrometer per second). This equation describes an overall response of the cell that is composed of a statistical superposition of invariant single-photon responses, each corresponding to a complete closure of the light-regulated conductance in a small region of the outer segment centered at the site of photon absorption (*6, 9, 13*). That is, the curves show the relation expected if there were no light adaptation, and fit well the experimental relations at these early times (100 and 150 ms) after light onset.

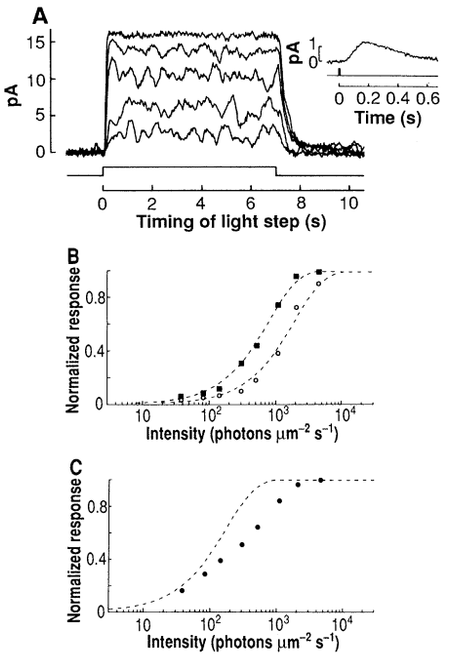

Fig. 1. (**A**) Family of responses to light steps of increasing intensity elicited from a cat rod. Timing of light step (7 s long) is indicated below the responses. In order to reduce photon fluctuations, each of the bottom four traces is from an average of two stimulus trials; the top trace is from a single trial. Step intensities were 82, 142, 503, 1074, and 2001 photons μm^{-2} s^{-1}, respectively. Temperature was 39°C. (Inset) Averaged response of the same cell in zero background to a dim flash delivering 6.5 photons μm^{-2}. (**B**) Normalized response-intensity relations for the step response family in (A), measured at 100 ms (○) and 150 ms (■) after the beginning of the light step. (**C**) Same kind of relation as in (B), except measured from mean steady-state levels of the responses. There are more intensity points in (B) and (C) than traces in (A) because only the responses to a few step intensities are shown in (A). The dashed curves in (B) and (C) are all drawn according to Eq. 1.

At the mean plateau levels of the responses, however, the experimental response-intensity relation rises much more gently than those at earlier times, indicating the presence of adaptation to light (Fig. 1C). Thus, adaptation developed progressively with time. The horizontal position of the zero-adaptation curve in Fig. 1C is determined by the relation $k_s = k_f t_i$ (*9*), where t_i is the integration time of the dim flash response of the cell (Fig. 1A, inset) and k_f is a constant denoting dim flash sensitivity (expressed as fractional response photon^{-1} μm^2) (*14*). This calculated position of the curve closely approaches the experimental relation at the lowest intensity, as expected from the minimal light adaptation at this dim light level. Six other experiments gave the same results, that is, significant deviation of the steady-state response-intensity relation from the zero-adaptation curve (Fig. 2). On average, the steady-state response reached half-maximum at a light intensity producing 180 ± 110 (SD) photoisomerizations (Rh*) per second and became fully saturated at about 4000 Rh* s^{-1} [both calculated with an effective collecting area of 0.35 μm^2 for the cat rod outer segments in our experiments (*15*)]. Our half-saturating light intensity is similar to an indirect estimate made by Nelson (*16*) from intracellular recordings of the rod input to cones, and the saturating intensity roughly agrees with earlier estimates from ganglion cell recordings (*17*) or the local electroretinogram (*18*), all in cat.

We also examined the sensitivity of the rods to incremental flashes superposed on background light (Fig. 3). At ~10 s after the onset of a background light, by which time the response of the cell to the background (Fig. 3A, left column) was already in steady state, incremental flashes were superposed on the light step with an intensity adjusted to elicit just-detectable responses. The averages of these incremental responses for different backgrounds are shown, at a higher gain, in Fig. 3A, right column. The averaged dim flash response elicited in the absence of background light is shown at the bottom. With increasing background intensity, the time-to-peak of the incremental flash responses shortened progressively, being reduced by about 40% at the brightest background compared to darkness.

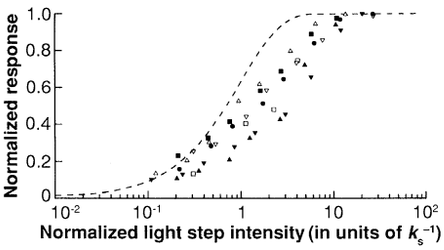

Fig. 2. Collected step response-intensity relations in steady state from seven cat rods, plotted on normalized axes. Dashed curve is drawn according to Eq. 1. For each cell, the position of the curve relative to the experimental points was determined by measurement of the response of the cell to dim flashes in the manner described in the text (that is, $k_s = k_f t_i$) before plotting on the normalized intensity axis (*14*). Saturated photocurrents ranged from 9.1 to 16.1 pA. Temperature was 39° to 40°C.

The reduction in flash sensitivity as a function of background intensity is shown Fig. 3B. The sensitivity reduction is expressed in the normalized form S_F/S_F^D, where S_F is the flash sensitivity in the presence of background light and S_F^D is the absolute flash sensitivity without background light. The solid curve is drawn according to $S_F/S_F^D = [1 + I_s/I_o]^{-1}$, where I_s is the steady background intensity and I_o is a constant equal to 67 photons μm^{-2} s^{-1} in this experiment. This is the familiar Weber-Fechner relation describing light adaptation, which applies to the behavior of rods in many lower vertebrates [(*5*), for example]. The dashed curve is drawn according to $S_F/S_F^D = e^{-k_s I_s}$, derived by differentiating Eq. 1 and representing the relation expected if there were no light adaptation (*9*). The indicated position of the dashed curve is again fixed by k_s, calculated from $k_s = k_f t_i$, with k_f and t_i obtained from the dim flash response of the cell in the absence of background light. Experiments with four separate rods gave similar results (Fig. 4), with an I_o (average ± SD) of 100 ± 31 photons μm^{-2} s^{-1} at 500 nm, corresponding to about 35 Rh* s^{-1}. Overall, we observed Weber-Fechner behavior in these cells with flash sensitivity down to 1/50 to 1/100 of control values. At higher background intensities, the steady response became too close to saturation for incremental flash sensitivity to be properly tested, but we expect this to decline precipitously, that is, much more steeply than a slope of −1. This Weber-Fechner range of desensitization is not very different from that observed with the same recording technique in lower vertebrates, such as the toad (*5, 19*). However, the I_o value is lower in the toad (about 4 to 10 Rh* s^{-1}), partly because of the longer (roughly sixfold as long) integration times of the single-photon responses in cold-

blooded animals due to the lower temperature (*20*).

We have observed a broadly similar behavior in rods of other mammals, including rabbit, cattle, rat, and several primate species (*20*). Reexamining past work by others, we find that Penn and Hagins (*8*) also observed a Weber-Fechner behavior in the rat rod, except, curiously, they concluded that this could be explained without invoking light adaptation (*21*). Steinberg (*22*) has also found a hint of Weber-Fechner behavior in cat pigment epithelial cells, a result that indirectly indicated rod activity. Finally, the observations made by Baylor *et al.* (*9*) on macaque rods did not rule out a small degree of adaptation in these cells.

We conclude from our results that mammalian rods can indeed adapt to light and probably use the same cellular mechanisms as do lower vertebrates (*13*). In fact, one also sees a need for rod adaptation, at least in animal species that have cone-sparse retinas. For example, the cat has far fewer cones than humans (*23, 24*), and its cone system has a higher threshold, corresponding to a white light level that already produces 50 to 400 Rh* s^{-1} in individual rods (*17*). Without adaptation, the cat rods would rapidly saturate at these light levels, before the cones could fully take over vision. The adaptability of the rods in the cat prevents such a discontinuity at the rod-cone transition. Indeed, it has been shown (*17, 25*) that cat vision in white light remains dominated by rods until a light level producing close to 10^3 Rh* s^{-1} in individual rods is reached. At this light intensity, the incremental flash sensitivity of the average cat rod without adaptation would have shown a 10^4-fold decrease compared to that in darkness (see Fig. 4). In contrast, light adaptation compromises the incremental sensitivity only slightly at low background levels, but allows the rod to reduce its gain by only 50-fold at 10^3 Rh* s^{-1}.

Nonetheless, network (that is, nonreceptor) adaptation (7) remains important in the rod pathway, even in the cat retina. With a high degree of convergence in the cat rod pathway (*24*), the absolute threshold for rod vision is determined by a large pooling of rod signals rather than by individual rods (*26*). Thus, the adaptation of the rod system at background intensities not far above the absolute threshold must also be a network phenomenon. In other words, the entire operating range of the rod system is composed of a lower intensity range set by network adaptation and a higher intensity range probably determined mostly by receptor adaptation, presumably as in lower vertebrates (*4, 27*).

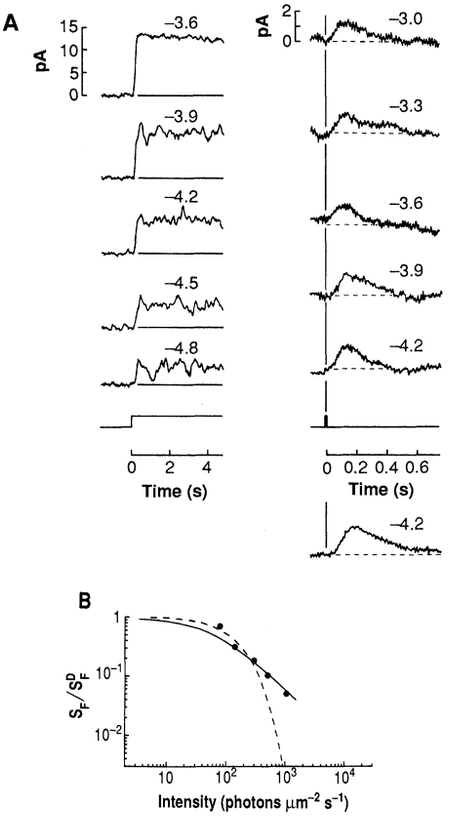

Fig. 3. (**A**) Incremental flash responses elicited from a cat rod in the presence of background light. (Left) The beginning of the background light steps and the corresponding responses from the cell. (Right) Averaged responses to the incremental flashes at different backgrounds, plotted at higher gain. Flash response at the bottom of the right column is the control elicited in the absence of background light. The number above each step or flash response indicates the log light attenuation used. Actual incremental flash intensities were 6.5 (no background), 6.5, 12, 24, 47, and 94 photons μm^{-2}; the corresponding flash responses were averages of 66, 20, 15, 15, 15, and 15 trials. Dashed lines indicate the baselines used for measuring response amplitudes. Temperature, 39°C. (**B**) Reduction in flash sensitivity plotted as a function of background light intensity, obtained from the experiment in (A). The incremental flash sensitivity measured at each of the two lowest background intensities was derived from averages of two flash intensities, only one of which is shown in (A). Continuous curve is drawn from $S_F/S_F^D = [1 + I_s/I_o]^{-1}$, while dashed curve is drawn from $S_F/S_F^D = e^{-k_s I_s}$. See text for details.

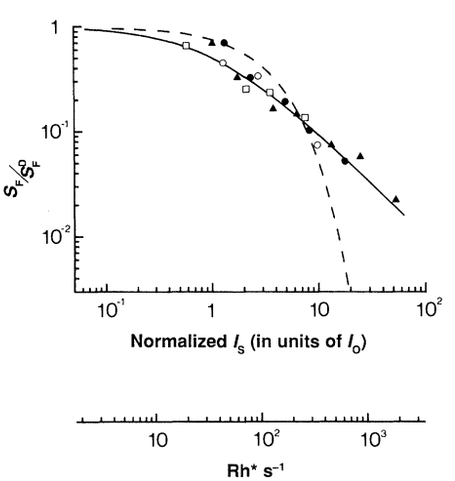

Fig. 4. Collected results from four incremental flash-on-background experiments, plotted on normalized axes. Continuous and dashed curves have same significance as in Fig. 3. The average value of I_o is about 35 Rh* s^{-1}, as shown on the lower horizontal scale. The position of the dashed curve relative to the experimental points represents the average position of such curves for all four cells.

REFERENCES AND NOTES

1. R. Shapley and C. Enroth-Cugell, in *Progress in Retinal Research*, N. N. Osborne and G. J. Chader, Ed. (Pergamon, Oxford, 1984), vol. 3, pp. 263–346; W. A. H. Rushton, *Proc. R. Soc. London Ser. B* **162**, 20 (1965); D. I. A. MacLeod, *Annu. Rev. Psychol.* **29**, 613 (1978); D. G. Green, *Vision Res.* **26**(*9*), 1417 (1986).
2. J. E. Dowling and H. Ripps, *J. Gen. Physiol.* **60**, 698 (1972); D. A. Baylor and A. L. Hodgkin, *J. Physiol. (London)* **242**, 729 (1974); J. A. Coles and S. Yamane, *ibid.* **247**, 189 (1975); J. Kleinschmidt and J. E. Dowling, *J. Gen. Physiol.* **66**, 617 (1975); S. Hemilä, *ibid.* **265**, 721 (1977); D. R. Copenhagen and D. G. Green, *ibid.* **369**, 161 (1985). A notable exception, however, is the mudpuppy rod, which is reported not to adapt to light [R. A. Normann and F. S. Werblin, *J. Gen. Physiol.* **63**, 37 (1974)]; nonetheless, a reexamination may be useful.
3. G. L. Fain, *J. Physiol. (London)* **261**, 71 (1976).
4. D. G. Green, J. E. Dowling, I. M. Siegel, H. Ripps, *J. Gen. Physiol.* **65**, 483 (1975).
5. D. A. Baylor, G. Matthews, K.-W. Yau, *J. Physiol. (London)* **309**, 591 (1980).
6. T. D. Lamb, P. A. McNaughton, K.-W. Yau, *ibid.* **319**, 463 (1981).
7. J. E. Dowling, *Science* **155**, 273 (1967); C. Enroth-Cugell and R. M. Shapley, *J. Physiol. (London)* **233**, 311 (1973); D. G. Green, *ibid.* **228**, 781 (1973); ——— and M. K. Powers, *Vision Res.* **22**, 209 (1982).
8. R. D. Penn and W. A. Hagins, *Biophys. J.* **12**, 1073 (1972).
9. D. A. Baylor, B. J. Nunn, J. L. Schnapf, *J. Physiol. (London)* **357**, 575 (1984).
10. E. N. Pugh, Jr., and J. Altman, *Nature* **334**, 16 (1988).
11. This saline solution contained (*9*) 140 m*M* NaCl, 3.6 m*M* KCl, 1.2 m*M* $CaCl_2$, 2.4 m*M* $MgCl_2$, 3 m*M* Na-Hepes, 10 m*M* dextrose, 0.02 m*M* Na-EDTA, *p*H 7.6.
12. K.-W. Yau, T. D. Lamb, D. A. Baylor, *Nature* **269**, 78 (1977); D. A. Baylor, T. D. Lamb, K.-W. Yau, *J. Physiol. (London)* **288**, 589 (1979).
13. H. R. Matthews, R. L. W. Murphy, G. L. Fain, T. D. Lamb, *Nature* **334**, 67 (1988); K. Nakatani and K.-W. Yau, *ibid.*, p. 69.
14. The dim flash response elicited in the absence of background (Fig. 1A, inset) had a peak amplitude of 1.35 pA. With the flash intensity calibrated to be 6.51 photons μm^{-2}, the flash sensitivity (S_F^D) was therefore 0.21 pA photon^{-1} μm^2. The averaged saturated photocurrent during the step response family in Fig. 1A was 13.9 pA. Thus $k_f = 0.015$ photon^{-1} μm^2. Finally, the integration time, t_i, of the dim flash response, defined as $\int r(t)dt/r_p$, where $r(t)$ is the response time course and r_p is the response peak [D. A. Baylor and A. L. Hodgkin, *J. Physiol. (London)* **234**, 163 (1973)], was 0.35 s. Thus $k_s = k_f t_i = 0.0052$ photon^{-1} μm^2 s. The dashed curve in Fig. 1C was therefore drawn according to $\hat{r}_s = 1 - e^{-0.0052 I_s}$.
15. For transverse illumination with unpolarized light, the effective collecting area A is given by [D. A. Baylor, T. D. Lamb, K.-W. Yau, *J. Physiol. (London)* **288**, 613 (1979)]: $A = \pi r^2 l \times Q_{isom} \times 0.5 \times 2.303\ \alpha$, where l is length of outer segment, r is radius, Q_{isom} is quantum efficiency of isomerization, and α is the specific axial pigment density. Taking

l = 25 μm, r = 0.6 μm (measured from the cat rod outer segments encountered in our experiments), Q_{isom} = 0.67 [H. J. A. Dartnall, in *Handbook of Sensory Physiology, Photochemistry of Vision*, H. J. A. Dartnall, Ed. (Springer-Verlag, Berlin, 1972), vol. VII/1, pp. 122–145] and α = 0.016 μm^{-1} for light at 500 nm [P. A. Liebman, *ibid.*, pp. 481–528; F. I. Harosi, *J. Gen. Physiol.* **66**, 357 (1975)], A is calculated to be 0.35 μm^2. Since there are regional variations in the rod outer segment dimensions in the cat retina [R. H. Steinberg, M. Reid, P. L. Lacy, *J. Comp. Neurol.* **148**, 229 (1973)], this area should be considered to be only approximate.
16. R. Nelson, *J. Comp. Neurol.* **172**, 109 (1977).
17. N. W. Daw and A. L. Pearlman, *J. Physiol. (London)* **201**, 745 (1969); C. Enroth-Cugell, B. G. Hertz, P. Lennie, *ibid.* **269**, 273 (1977).
18. R. W. Rodieck and R. W. Ford, *Vision Res.* **9**, 1 (1969).
19. Many of the studies on rod adaptation in lower vertebrates were made with intracellular recordings. In these studies, the observed Weber-Fechner behavior of rod desensitization [see, for example, (*3*)] extends over a broader range of background intensities than measured with the suction-pipette method (*5*). This difference suggests that voltage-sensitive conductances at the rod inner segment, which shape the voltage response of the cell to light, may contribute to background adaptation by extending the Weber-Fechner range.
20. K. Nakatani, T. Tamura, K.-W. Yau, manuscripts in preparation.
21. Penn and Hagins suggested that simple response compression according to the Michaelis relation (given by the form $\hat{r} = I/(I + \sigma)$, where $\hat{r}$ is normalized response amplitude, I is light intensity, and σ is a constant) could directly lead to the Weber-Fechner type of desensitization. This is unlikely, however, because this relation should predict a flash sensitivity that decreases as the square of background intensity (which can be seen by differentiating the above relation with respect to I), rather than as the first power of I as in the Weber-Fechner relation. See also E. H. Adelson, *Vision Res.* **22**, 1299 (1982).
22. R. H. Steinberg, *J. Physiol. (London)* **217**, 93 (1971).
23. ———, M. Reid, P. L. Lacy, *J. Comp. Neurol.* **148**, 229 (1973).
24. P. Sterling, *Annu. Rev. Neurosci.* **6**, 149 (1983); ———, M. A. Freed, R. G. Smith, *J. Neurosci.* **8**, 623 (1988).
25. H. B. Barlow and W. R. Levick, *J. Physiol. (London)* **196**, 2P (1968); P. Hammond and C. R. James, *ibid.* **216**, 99 (1971); R. W. Rodieck and W. A. H. Rushton, *ibid.* **254**, 759 (1976).
26. H. B. Barlow, W. R. Levick, M. Yoon, *Vision Res. Suppl.* **3**, 87 (1971).
27. J. E. Dowling, *The Retina: An Approachable Part of the Brain* (Belknap-Harvard, Cambridge, 1987).
28. We thank M. L. Hudak and M. B. Sachs for kindly providing us with the cats at the end of their experiments, N. W. Daw for discussion, and L. W. Haynes and B. Minke for comments on the manuscript. Supported by a grant from the U.S. National Eye Institute. K.-W. Y. is an investigator of the Howard Hughes Medical Institute.

29 March 1989; accepted 12 June 1989

Limbic Seizures Increase Neuronal Production of Messenger RNA for Nerve Growth Factor

CHRISTINE M. GALL* AND PAUL J. ISACKSON

Nerve growth factor (NGF) produced by telencephalic neurons provides critical trophic support for cholinergic neurons of the basal forebrain. In situ hybridization and nuclease protection analyses demonstrate that limbic seizures dramatically increase the amount of messenger RNA for NGF in the neurons of the hippocampal dentate gyrus within 1 hour of seizure onset and in broadly distributed neocortical and olfactory forebrain neurons some hours later. The increased messenger RNA species is indistinguishable from messenger RNA for transcript B of the β subunit of NGF from mouse submandibular gland. Thus, the expression of a known growth factor is affected by unusual physiological activity, suggesting one route through which trophic interactions between neurons in adult brain can be modified.

NERVE GROWTH FACTOR, WHICH promotes the growth and maintenance of sympathetic and sensory neurons of the peripheral nervous system (*1*), is differentially expressed in the mammalian brain with the highest levels of NGF mRNA present in hippocampus (*2*). NGF synthesized by forebrain neurons may provide critical trophic support for cholinergic neurons of the basal forebrain, and disturbances in this relation may be involved in age-related neuropathologies such as Alzheimer's disease (*3, 4*). In support of this idea, it has been demonstrated that NGF is retrogradely transported from hippocampus to cholinergic neurons in septum and basal forebrain (*5*), and that infusion of NGF can prevent the degeneration of these same cholinergic cells after transection of their connections with hippocampus (*6*). Here we report that limbic seizures cause a rapid and pronounced increase in the expression of mRNA for NGF in the granule cells of the rat hippocampus. Moreover, a delayed increase was found in cortical areas, suggesting that the spread of seizure activity triggers changes in the expression of NGF mRNA throughout much of the forebrain.

Adult (280 to 350 g) male Sprague-Dawley rats (Simonsen Labs) were used. Recurrent limbic seizures were induced by the placement of a unilateral electrolytic lesion in the dentate gyrus hilus (*7*). Such lesions produce bilateral epileptiform electroencephalogram (EEG) activity in the hippocampus and behavioral seizures of the limbic kindling type (*8*) without causing secondary neuronal degeneration in the contralateral hippocampus. Hippocampal paroxysmal discharges begin 1.5 to 2 hours after the lesion and recur intermittently for 8 to 10 hours. Paired control rats received either ketamine-xylazine anesthesia alone or were anesthetized with sodium pentobarbital (50 mg/kg), and a lesion was placed in the dentate gyrus hilus with an insulated platinum-iridium wire. Such platinum wire lesions do not produce hippocampal EEG or behavioral seizures (*9*).

For in situ hybridization, experimental animals with behaviorally verified seizures and paired control rats were killed 2.5 (n = 1), 3 (n = 9), 4 (n = 3), 5 (n = 2), 6 to 7 (n = 5), 10 (n = 2), 17 (n = 3), and 24 (n = 5) hours after surgery by overdose with sodium pentobarbital and intracardial perfusion with 4% paraformaldehyde in 0.1M phosphate buffer (pH 7.4) (*10*). In the greater number of these studies, ^{35}S-labeled RNA probes complementary to the coding regions for either mature mouse (*11, 12*) (Fig. 1A) or rat β-NGF (*13*) were used. We have obtained qualitatively identical results with a 550-base RNA probe prepared from the 5′ end of a guinea pig β-NGF cDNA clone (*14*). Although similar seizure-induced changes in hybridization to NGF mRNA were observed bilaterally, the description here will be limited to regions contralateral to lesion placement. Controls for the specificity of hybridization included treatment of tissue sections with ribonuclease A before normal hybridization and hybridization of sections with labeled "sense" RNA sequences (*15*). No cellular labeling was observed in tissue from experimental or anesthetic-control rats processed under either control condition.

In untreated rats, in situ hybridization to NGF mRNA is greatest in the hippocampal formation. In tissue autoradiograms, subpopulations of neurons within the dentate gyrus hilus (Fig. 2A) and scattered within and around stratum pyramidale of hippocampus proper and subiculum were moderately densely labeled with the ^{35}S-labeled cRNA probe. As could be seen most clearly in tissue processed with the rat β-NGF cRNA sequence, stratum granulosum was also labeled, but with lower densities of autoradiographic grains. This distribution is essentially in agreement with other reports (*13, 16*), although we observed greater differences in the densities of hybridization to

C. M. Gall, Department of Anatomy and Neurobiology, University of California, Irvine, CA 92717.
P. J. Isackson, Department of Anatomy and Neurobiology, and Department of Biological Chemistry, University of California, Irvine, CA 92717.

*To whom correspondence should be addressed.